

NO-1886 upregulates ATP binding cassette transporter A1 and inhibits diet-induced atherosclerosis in Chinese Bama minipigs

Chi Zhang,^{*,†,§} Weidong Yin,^{1,*,†} Duanfang Liao,^{**} Liang Huang,^{††} Chaoke Tang,^{*} Kazuhiko Tsutsumi,^{§§} Zongbao Wang,[†] Yi Liu,[†] Qinkai Li,[†] Hongjie Hou,[†] Manbo Cai,[†] and Junxia Xiao[†]

Institute of Cardiovascular Research,^{*} Nanhua University Medical School, Hengyang, Hunan 421001, China; Department of Biochemistry and Molecular Biology,[†] Nanhua University School of Life Sciences and Technology, Hengyang, Hunan 421001, China; Function Laboratory Center,[§] Nanhua University Medical School, Hengyang, Hunan 421001, China; Institute of Pharmacy and Pharmacology,^{**} Nanhua University, Hengyang, Hunan 421001, China; Department of Operative Surgery,^{††} Nanhua University Medical School, Hengyang, Hunan 421001, China; and Research and Development,^{§§} Otsuka Pharmaceutical Factory, Inc., Tokushima, Japan

Abstract It is widely believed that high density lipoprotein-cholesterol (HDL-C) functions to transport cholesterol from peripheral cells to the liver by reverse cholesterol transport (RCT), a pathway that may protect against atherosclerosis by clearing excess cholesterol from arterial cells. A cellular ATP binding cassette transporter called ABCA1 mediates the first step of RCT. NO-1886 has been proven to be highly effective at increasing HDL-C and reducing atherosclerosis. However, the mechanism of atherosclerosis inhibition for NO-1886 is not fully understood. In this study, the effects of NO-1886 on ABCA1 were investigated in high-fat/high-sucrose/high-cholesterol-fed Chinese Bama minipigs. Administration of NO-1886 (0.1 g/kg body weight/day) in the diet for 5 months significantly reduced atherosclerosis lesions and significantly increased plasma HDL-C and apolipoprotein A-I levels. The mRNA and protein levels of ABCA1 in the liver, retroperitoneal adipose tissue, and aorta were increased by NO-1886 as well. Multivariate linear regression analysis showed that the levels of LPL in plasma and the levels of ABCA1 in aorta were independently associated with the atherosclerotic lesion area. In addition, NO-1886 upregulated liver X receptor α and affected the expression of scavenger receptor class B type I in the liver. **These results demonstrate that the mechanism of atherosclerosis inhibition for NO-1886 is associated with its effect on ABCA1.**—Zhang, C., W. Yin, D. Liao, L. Huang, C. Tang, K. Tsutsumi, Z. Wang, Y. Liu, Q. Li, H. Hou, M. Cai, and J. Xiao. **NO-1886 upregulates ATP binding cassette transporter A1 and inhibits diet-induced atherosclerosis in Chinese Bama minipigs.** *J. Lipid Res.* 2006. 47: 2055–2063.

Supplementary key words liver X receptor α • scavenger receptor class B type I • [4-(4-bromo-2-cyano-phenylcarbamoyl)-benzyl]phosphonic acid diethyl ester

Tsutsumi et al. (1) reported that a novel compound, NO-1886, possesses a potent LPL-enhancing activity. Administration of NO-1886 increased LPL activity in the post-heparin plasma, adipose tissue, and myocardium in rats, with a concomitant reduction in plasma triglyceride (TG) level and increase of high density lipoprotein-cholesterol (HDL-C) level (2). LPL hydrolyzes chylomicron and VLDL to remnants and LDL, whereas cholesterol, apolipoproteins, and surface phospholipids released from TG-rich lipoproteins fuse with smaller HDL particles, forming mature cholesterol-rich HDL particles. A negative relationship has been observed between the HDL-C concentration and the extent of atherosclerosis in many studies (3–5). One explanation for this protective effect of HDL against atherosclerosis is reverse cholesterol transport (RCT), the process by which cholesterol is removed from extrahepatic tissues and returned to the liver for conversion into bile acids and excretion into bile.

The first crucial step in the RCT pathway is the movement of excess cellular cholesterol and phospholipid from cell membranes to nascent HDL particles (6, 7). ABCA1 plays a key role in this step. Subsequently, HDL particles act in conjunction with the cholesterol-esterifying enzyme, lecithin:cholesterol acyltransferase. Cholesteryl ester accumulating in HDL then is involved in a number of different fates: uptake in the liver in HDL containing apolipo-

Manuscript received 29 December 2005 and in revised form 22 May 2006 and in re-revised form 28 June 2006.

Published, *JLR Papers in Press*, June 28, 2006.
DOI 10.1194/jlr.M600226-JLR200

Copyright © 2006 by the American Society for Biochemistry and Molecular Biology, Inc.

This article is available online at <http://www.jlr.org>

¹ To whom correspondence should be addressed:
e-mail wdy20012001@yahoo.com

protein by LDL receptors, selective uptake of HDL-cholesteryl ester in the liver or other tissues involving scavenger receptor class B type I (SR-BI), and transfer to TG-rich lipoproteins as a result of the activity of cholesteryl ester transfer protein, with subsequent uptake of TG-rich lipoprotein remnants in the liver (8).

NO-1886 has a role in reducing atherosclerosis. Because this compound increases HDL-C level and HDL-C is atheroprotective as a result of its role in RCT, we suppose that the mechanism of atherosclerosis inhibition for NO-1886 is related to the gatekeeper of the RCT pathway, ABCA1. In this study, we investigated the effects of NO-1886 on ABCA1 in high-fat/high-sucrose/high-cholesterol-fed Chinese Bama minipigs.

MATERIALS AND METHODS

Materials

NO-1886 ([4-(4-bromo-2-cyano-phenylcarbamoyl)-benzyl]-phosphonic acid diethyl ester; Chemical Abstracts Service (CAS) 133208-93-2; lot No. C00C99) was synthesized in the New Drug Research Laboratory of Otsuka Pharmaceutical Factory, Inc. (Tokushima, Japan). Sucrose was obtained from Liuzhou Sugar Co. (Guangxi, China), and lard was obtained from Hengyang Meat Products Co. (Hunan, China). Cholesterol was obtained from Sigma-Aldrich (>99% pure; St. Louis, MO).

Animals and diets

Male Chinese Bama minipigs, 2 months of age, were obtained from the barrier unit at the Laboratory Animal Center of Chongqing Medical University (Chongqing, China). Animals were randomized into four groups with similar body weight ($n = 7$ in the normal diet-fed group; $n = 7$ in the normal diet plus NO-1886 group; $n = 8$ in the high-fat/high-sucrose/high-cholesterol-fed group; $n = 8$ in the high-fat/high-sucrose/high-cholesterol-fed plus supplemented NO-1886 group). The high-fat/high-sucrose/high-cholesterol diet used in this study was normal pig diet supplemented with 10% lard, 37% sucrose, and 2% cholesterol, which was similar to a "diabetogenic" and "atherogenic" diet (1, 9). (The compositions of the diets are described in **Table 1**.) Animals were housed in single pens under controlled conditions (temperature between 18°C and 22°C, relative air humidity

30–70%, with four air changes per hour) and fed three times daily on a restricted schedule with normal control diet (CD), normal diet plus NO-1886 (CD1886), high-fat/high-sucrose/high-cholesterol diet (HFSCD), or high-fat/high-sucrose/high-cholesterol supplemented NO-1886 diet (HFSCD1886). All pigs received the same amount of food (4.0% body weight). The dose of NO-1886 administered for the CD1886 and HFSCD1886 groups was 0.1 g/kg body weight/day. The total study period was 5 months. Blood samples for plasma lipids and glucose inspection were obtained without sedation by pricking an ear vein with a lancet and collecting drops in a hematocrit tube at the end of each month after fasting overnight. The animals were euthanized at the end of month 5. The liver, retroperitoneal adipose tissue, and aorta were dissected free from adjacent tissues and frozen in liquid nitrogen. Institutional guidelines for animal care and use were followed.

Plasma measurement

Glucose, total cholesterol (TC), HDL-C, and TG were determined by commercial enzymatic methods (test kits from Shanghai Rongsheng Biotech, Inc., Shanghai, China). Plasma FFAs was measured by a colorimetric method (kits supplied by Nanjing Jianchen Biotech, Inc., Nanjing, China). Apolipoprotein A-I (apoA-I) was measured by immunoturbidimetry (test kits from Shanghai Rongsheng Biotech). LPL activity in postheparin plasma was measured by an immunochemical method described previously (10). Then, heparin (150 U/kg) was injected into the femoral vein, and 10 min later blood was collected, the plasma was separated by centrifugation at 1,000 *g* for 15 min, and the glycerol tri[¹⁴C]oleate was used as a substrate for selective blocking of hepatic lipase activity with antiserum to rat hepatic lipase.

Morphological examination of atherosclerotic lesions

At the end of the experimental period, the animals were euthanized by phlebotomy under light anesthesia with sodium pentobarbital (30 mg/kg iv; Jilin Northern Medicine, Inc.). Atherosclerotic lesions were analyzed by a method described previously (11). The aorta was dissected from the aortic valve to the iliac bifurcation, and as much adventitia as possible was removed to prevent errors during Sudan IV staining of the vessel. The aorta was opened longitudinally and pinned flat on a Styrofoam surface. After overnight fixation in 10% formalin, the aorta was rinsed in 70% ethanol for 10 min and then stained with 0.5% Sudan IV in 35% ethanol and 50% acetone for 20 min. Destaining was carried out for 20 min in 80% ethanol. Lipid deposition in the aorta was determined by morphological assessment of the percentage of lesion-covered aorta as visualized by Sudan IV staining of the region between the aortic root and the bifurcation. Fatty streak lesions on enlarged photographs were traced on a digital tablet, and atherosclerotic lesions were analyzed using image-analysis software (NIH Image). The aortic lesion area was calculated as a percentage as follows: atherosclerotic lesion area ÷ area of the aorta × 100.

Biochemical analysis of the artery wall

Because all aortas were fixed and stained for fatty streak lesion determination, they were not suitable for chemical analysis; therefore, common carotid arteries were used for cholesterol and cholesteryl ester analyses to determine the effect of NO-1886 on arterial lipid deposition. It has been shown that fatty streak lesions in the common carotid artery develop similarly to those in the aorta. Therefore, 30 common carotid arteries were washed in ice-cold saline, blotted dry between sheets of filter paper, and weighed. Cholesterol and cholesteryl ester contents

TABLE 1. Components of the diets

Component	Control Diet	High-Fat/High-Sucrose/ High-Cholesterol Diet
		%
Rice	64.11	31.98
Wheat bran	10.51	5.57
Soybean meal	11.98	6.35
Cottonseed meal	4	2.12
Colza meal	4	2.12
Fish powder	2	1
Bone powder	1.1	0.5
Calcium bicarbonate	0.8	0.8
Salt	0.5	0.5
Trace elements	0.5	0.5
Vitamins	0.5	0.5
Pork lard		10
Sucrose		37
Cholesterol		2

in the arteries were measured after they were homogenized in phosphate buffer, and the lipid was extracted from the homogenates as described by Folch, Lees, and Sloane Stanley (12); quantitative gas-liquid chromatography was performed as described by Rapp et al. (13). The samples were analyzed for free cholesterol before and after saponification, and the calculated difference represents the cholesteryl ester concentration. Cholesterol (Sigma-Aldrich) was used as a standard for free cholesterol determinations.

RNA preparation and real-time quantitative RT-PCR

Real-time quantitative RT-PCR was performed to determine the relative expression levels of ABCA1 in minipig tissues. Total RNA was extracted from liver, retroperitoneal adipose tissue, and aorta using RNA extraction Trizol reagent (Invitrogen). After contaminated genomic DNA was digested with DNase I (Roche Diagnostics), first standard cDNA was synthesized using a SuperScript™ preamplification system (Invitrogen) from 2 µg of total RNA. PCR was performed using primers (sense and antisense) for cDNA 5'-GGG GTG GTG TTC TTC CTC ATT-3' and 5'-CAG GCT TCC GCT TCC TTC TAT-3' (for ABCA1) and 5'-CCT GTA CGC CAA CAC AGT GC-3' and 5'-ATA CTC CTG CTT GCT GAT CC-3' (for β-actin) (synthesized by Sangon Technology Co., Ltd.). Primers were validated by analysis of template titration and dissociation curves. Each reaction (50 µl) contained 0.3 µmol/l primers, 25 µl of 2× SYBR Green PCR master mix reagent, and 2 µl of template and was amplified by 40 cycles of denaturation (94°C, 30 s), annealing (60°C, 30 s), and extension (72°C, 30 s). The quantification of ABCA1 and β-actin mRNA was achieved in an ABI PRISM 7700 sequence detection system (Applied Biosystems) and analyzed using ABI PRISM sequence detector software (version 1.6.3; Applied Biosystems). Transcript levels were normalized to the amount of β-actin transcript. Standard curves were generated for target genes and compared with β-actin using serial dilutions of mRNA, and they were found to be linear from 0.08 to 50 ng of RNA in the reaction mixture. This range included the effective concentrations used in the experiments. Melting curve analysis was performed to confirm the production of a single product in these reactions. All analyses were performed in triplicate.

Protein isolation and Western blotting

Protein was isolated from flash-frozen minipig liver, retroperitoneal adipose tissue, and aorta samples as described previously (14). Total protein (10–50 µg/lane) was electrophoresed and separated on a 6–10% SDS-polyacrylamide gel and transferred to a nitrocellulose membrane (Hybond-C; Amersham), which was soaked in 5% nonfat dry milk in Tris-Buffered Saline Tween (TBST) (pH 7.6). Membranes were incubated overnight with a rabbit polyclonal antibody to human ABCA1 (Novus Biologicals) at a dilution of 1:500 on a rotating platform at 4°C, a rabbit polyclonal antibody to human liver X receptor α (LXRα; Novus Biologicals) at a dilution of 1:400 on a rotating platform at 4°C, or a rabbit polyclonal antibody to human SR-BI (Novus Biologicals) at a dilution of 1:1,000 on a rotating platform at 4°C. Subsequently, membranes were rinsed in TBST (pH 7.6) and incubated with horseradish peroxidase-conjugated anti-rabbit IgG antibodies (Zymed Laboratories) diluted in TBST (1:2,000) for 1 h on a rotating platform at 4°C. Bands were visualized using a HRP developer, and background-subtracted signals were quantified on a laser densitometer (Bio-Rad). Blots were probed with mouse anti-β-actin monoclonal antibody (Sigma-Aldrich) to ensure equal protein loading. All protein levels were assessed by densitometry with β-actin used as a control.

Statistical analysis

Results are expressed as means ± SD. Statistical analysis was performed using the MANOVA. Statistical significance was obtained at $P < 0.05$. Multivariate linear regression analysis was used to evaluate the relationship among levels of ABCA1, SR-BI, LPL, and lesion areas of the aorta in HFSCD-fed minipigs. For non-quantitative data, results are representative of at least three independent experiments.

RESULTS

Postheparin plasma LPL activity

NO-1886 supplementation caused a marked increase in postprandial postheparin plasma LPL activity [47.6 ± 5.4 nmol/ml/min in the HFSCD1886 group vs. 31.9 ± 8.1 nmol/ml/min in the HFSCD group ($P < 0.01$); 16.4 ± 4.2 nmol/ml/min in the CD1886 group vs. 7.3 ± 1.7 nmol/ml/min in the CD group ($P < 0.05$)]. NO-1886 supplementation also increased fasting plasma LPL activity in pigs from both the HFSCD1886 and CD1886 groups, even though there is no statistical difference between HFSCD1886 and HFSCD, and between the CD1886 and CD groups (Table 2).

Plasma TC

Plasma TC level was significantly increased in the HFSCD and HFSCD1886 groups over the control groups by the 1st month of feeding and remained that way for the duration of the study. NO-1886 also slightly increased plasma TC when normal diet was added to the drug in the process of the experiment. No overall difference in plasma TC was detected between the HFSCD and HFSCD1886 groups. In the 1st and 2nd months, administration of NO-1886 in the HFSCD group caused an increase of plasma TC, even higher than in the HFSCD1886 group. We believe that this was because of an increase of plasma HDL-C level, which was increased significantly by NO-1886 (Table 3).

Plasma HDL-C and apoA-I

HDL-C levels in HFSCD groups fed with and without NO-1886 were increased linearly with time. A significant increase in HDL-C was observed as early as at the end of the 1st month compared with the control group (HFSCD group, 1.07 ± 0.16 mmol/l; HFSCD1886 group, 1.23 ± 0.24 mmol/l vs. 0.80 ± 0.16 mmol/l in the control group).

TABLE 2. Postheparin plasma LPL activity

Conditions	HFSCD1886	HFSCD	CD1886	CD
Postprandial	$47.6 \pm 9.6^{a,b}$	31.9 ± 8.1^a	16.4 ± 4.2^a	7.3 ± 1.7
Fasting	9.3 ± 2.7^a	8.6 ± 1.8^a	5.6 ± 1.1	4.1 ± 0.8

CD, control diet; CD1886, control diet plus NO-1886; HFSCD, high-fat/high-sucrose/high-cholesterol diet; HFSCD1886, HFSCD diet plus NO-1886. Values shown are nmol/ml/min. $n = 7$ for the CD and CD1886 groups, and $n = 8$ for the HFSCD and HFSCD1886 groups.

^a $P < 0.05$ versus the CD group.

^b $P < 0.05$ versus the HFSCD group.

TABLE 3. Fasting plasma lipid and glucose concentrations

Parameter	Time 0	1 Month	2 Months	3 Months	4 Months	5 Months
TC (mmol/l)						
CD	2.1 ± 0.4	2.0 ± 0.3	1.9 ± 0.3	1.7 ± 0.3	1.8 ± 0.5	2.1 ± 0.5
CD1886	2.1 ± 0.5	2.0 ± 0.4	2.2 ± 0.4	2.0 ± 0.5	2.0 ± 0.5	2.6 ± 0.6
HFSCD	2.2 ± 0.5	6.3 ± 1.4 ^a	9.1 ± 1.2 ^a	11.2 ± 2.3 ^a	14.9 ± 1.7 ^a	20.5 ± 3.3 ^a
HFSCD1886	2.3 ± 0.5	7.9 ± 1.9 ^b	11.2 ± 2.2 ^c	12.8 ± 3.0	16.2 ± 3.4	21.4 ± 4.0
High density lipoprotein (mmol/l)						
CD	0.77 ± 0.12	0.80 ± 0.16	0.87 ± 0.15	0.99 ± 0.12	0.87 ± 0.15	0.94 ± 0.23
CD1886	0.82 ± 0.12	0.85 ± 0.18	1.12 ± 0.37	1.40 ± 0.33 ^d	1.34 ± 0.30 ^d	1.36 ± 0.28 ^d
HFSCD	0.78 ± 0.12	1.07 ± 0.16 ^d	1.41 ± 0.31 ^a	1.81 ± 0.44 ^a	1.96 ± 0.45 ^a	1.94 ± 0.45 ^a
HFSCD1886	0.79 ± 0.15	1.23 ± 0.24	2.41 ± 0.38 ^c	2.87 ± 0.47 ^c	3.01 ± 0.46 ^c	2.86 ± 0.46 ^c
Apolipoprotein A-I (g/l)						
CD	0.098 ± 0.020	0.102 ± 0.021	0.094 ± 0.023	0.094 ± 0.044	0.089 ± 0.036	0.105 ± 0.027
CD1886	0.103 ± 0.017	0.107 ± 0.018	0.114 ± 0.024	0.126 ± 0.041	0.198 ± 0.047 ^d	0.188 ± 0.044
HFSCD	0.100 ± 0.020	0.360 ± 0.105 ^a	0.415 ± 0.116 ^a	0.557 ± 0.132 ^a	0.504 ± 0.085 ^a	0.519 ± 0.084 ^a
HFSCD1886	0.094 ± 0.015	0.471 ± 0.092 ^c	0.528 ± 0.106 ^b	0.719 ± 0.164 ^c	0.705 ± 0.127 ^c	0.756 ± 0.125 ^c
TC/HDL ratio						
CD	2.8 ± 0.8	2.6 ± 0.6	2.3 ± 0.5	1.8 ± 0.3	2.3 ± 0.9	2.3 ± 0.7
CD1886	2.6 ± 0.6	2.4 ± 0.6	2.1 ± 0.5	1.5 ± 0.3	1.5 ± 0.3	2.0 ± 0.7
HFSCD	2.6 ± 0.7	6.0 ± 1.7 ^a	6.7 ± 1.6 ^a	6.4 ± 1.5 ^a	7.3 ± 1.4 ^a	10.4 ± 2.9 ^a
HFSCD1886	3.0 ± 1.1	6.5 ± 1.3	4.8 ± 1.4 ^c	4.5 ± 0.8 ^c	5.3 ± 0.5 ^c	7.3 ± 1.2 ^c
Triglyceride (mmol/l)						
CD	0.59 ± 0.05	0.60 ± 0.05	0.63 ± 0.08	0.68 ± 0.14	0.69 ± 0.12	0.72 ± 0.13
CD1886	0.57 ± 0.05	0.41 ± 0.08 ^a	0.42 ± 0.09 ^a	0.44 ± 0.08 ^a	0.44 ± 0.09	0.44 ± 0.06 ^d
HFSCD	0.59 ± 0.04	0.97 ± 0.11 ^a	1.50 ± 0.20 ^a	1.87 ± 0.18 ^a	1.90 ± 0.36 ^a	2.10 ± 0.25 ^a
HFSCD1886	0.58 ± 0.05	0.60 ± 0.03 ^c	0.75 ± 0.13 ^c	0.89 ± 0.17 ^c	1.01 ± 0.20 ^c	1.09 ± 0.25 ^c
Free fatty acids (mmol/l)						
CD	0.111 ± 0.024	0.222 ± 0.040	0.240 ± 0.035	0.281 ± 0.037	0.288 ± 0.056	0.293 ± 0.045
CD1886	0.112 ± 0.014	0.196 ± 0.090	0.231 ± 0.046	0.285 ± 0.059	0.289 ± 0.059	0.294 ± 0.053
HFSCD	0.110 ± 0.021	0.253 ± 0.055	0.315 ± 0.048 ^a	0.759 ± 0.166 ^a	0.998 ± 0.176 ^a	0.982 ± 0.247 ^a
HFSCD1886	0.136 ± 0.041	0.193 ± 0.042	0.253 ± 0.031 ^c	0.366 ± 0.092 ^c	0.450 ± 0.124 ^c	0.393 ± 0.076 ^c
Glucose (mmol/l)						
CD	4.7 ± 0.5	4.5 ± 0.8	4.8 ± 0.7	5.2 ± 0.9	4.7 ± 0.8	4.9 ± 0.5
CD1886	4.8 ± 0.6	4.7 ± 0.8	4.5 ± 0.6	4.5 ± 1.0	5.0 ± 1.0	4.7 ± 0.7
HFSCD	4.8 ± 0.8	5.9 ± 0.9 ^d	7.3 ± 1.8 ^a	9.1 ± 2.0 ^a	9.7 ± 2.3 ^a	10.1 ± 2.3 ^a
HFSCD1886	4.9 ± 0.9	4.7 ± 1.7 ^b	5.0 ± 1.2 ^c	6.1 ± 1.1 ^c	5.3 ± 1.2 ^c	5.5 ± 1.2 ^c

TC, total cholesterol. Values shown are means ± SD. n = 7 for the CD and CD1886 groups, and n = 8 for the HFSCD and HFSCD1886 groups.

^a *P* < 0.01 versus the CD group.

^b *P* < 0.05 versus the HFSCD group.

^c *P* < 0.01 versus the HFSCD group.

^d *P* < 0.05 versus the CD group.

Furthermore, the HFSCD1886 group had a statistically significantly higher level of HDL-C from month 2 compared with the HFSCD group and remained so for the duration. NO-1886 administered to normal diet-fed animals also caused an increase of HDL level in the CD1886 group (1.40 ± 0.33 mmol/l in the CD1886 group vs. 0.99 ± 0.12 mmol/l in the CD group at the end of month 3; *P* < 0.05) (Table 3). The changing patterns of plasma apoA-I were similar to those of HDL-C. Additionally, apoA-I levels increased gradually and significantly in NO-1886-supplemented groups (Table 3).

Plasma TC/HDL-C ratio

The TC/HDL-C ratio predicts coronary heart disease risk regardless of the absolute TC and HDL-C. We detected that plasma TC/HDL-C ratio decreased in NO-1886 supplemental groups. As shown in Table 3, the plasma TC/HDL-C ratio data suggested that the increase in plasma TC in NO-1886-supplemental groups was primarily a reflection of an increase in HDL-C.

Plasma TG

Plasma TG concentrations were significantly increased in miniature pigs fed the HFSCD from the 2nd month of experimentation, and this persisted for the remainder of the study period and reached a plateau at month 5. Administration of NO-1886 markedly decreased plasma TG (1.09 ± 0.25 mmol/l in the HFSCD1886 group vs. 2.10 ± 0.25 mmol/l in the HFSCD group; *P* < 0.01) (Table 3). Similarly, plasma TG was 0.44 ± 0.06 mmol/l in the CD1886 group versus 0.72 ± 0.13 mmol/l in the CD group at the 5th month (*P* < 0.05; Table 3).

Plasma FFA

There was no difference in plasma free fatty acid among the four groups before the start of the experiment. However, FFA levels in the HFSCD group increased rapidly at the end of month 3, which was 2.4-fold higher than that in the control group, and increased gradually during the months left. Supplementation with NO-1886 significantly decreased the level of FFA approximately to that of the

control group (0.393 ± 0.076 mmol/l in the HFSCD1886 group vs. 0.982 ± 0.247 mmol/l for the HFSCD group; $P < 0.01$), but there was no statistical difference between the CD1886 group and the CD group (Table 3).

Plasma glucose

Plasma glucose concentration in HFSCD-fed animals was increased linearly with time and reached a plateau of 10.1 ± 2.3 mmol/l at month 5, which was 1.0-fold higher than that in the CD group. Administration of NO-1886 markedly decreased the level of plasma glucose (5.5 ± 1.2 mmol/l in the HFSCD1886 group vs. 10.1 ± 2.3 mmol/l in the HFSCD group; $P < 0.01$) (Table 3).

Effect of NO-1886 on fatty streak formation

As shown in Fig. 1, the aortas were prone to develop fatty streak lesions in HFSCD-fed pigs. Relative aortic fatty streak lesion area was $43.6 \pm 12.8\%$ for the HFSCD group and $16.4 \pm 8.2\%$ for the HFSCD1886 group ($P < 0.01$). Thus, supplementing NO-1886 into the high-fat/high-sucrose/high-cholesterol diet resulted in a remarkable amelioration in aortic fatty streak lesions. No fatty streak was observed in aortas of the pigs from the CD1886 and CD groups.

Chemical analysis of common carotid arteries

To further evaluate the extent of atherosclerosis, common carotid arteries from four dietary groups were analyzed for TC and cholesteryl ester deposition (Fig. 2). TC contents of the arteries were 76.7% higher in the HFSCD group than in pigs from the HFSCD1886 group ($P < 0.01$), and cholesteryl ester levels were also increased by 97.8% ($P < 0.01$) in the HFSCD group. Free cholesterol content in the common carotid artery was increased modestly by 52.7% in the HFSCD group ($P < 0.05$).

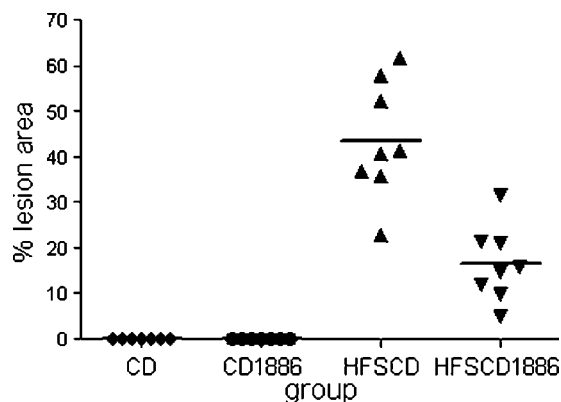


Fig. 1. Scatterplot showing lesion areas on the abdominal portion of the aorta of Chinese Bama miniature pigs fed the control diet (CD; diamonds), the control diet plus NO-1886 (CD1886; circles), the high-fat/high-sucrose/high-cholesterol diet (HFSCD; triangles), or the HFSCD diet plus NO-1886 (HFSCD1886; inverted triangles). $n = 7$ for the CD and CD1886 groups, and $n = 8$ for the HFSCD and HFSCD1886 groups.

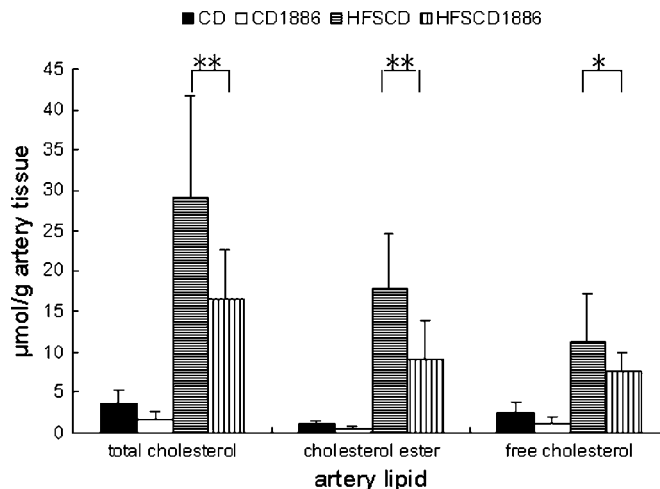


Fig. 2. Bar graphs showing cholesterol and cholesteryl ester deposition in the common carotid arteries of pigs fed CD, CD1886, HFSCD, or HFSCD1886 for 5 months. Data are expressed as means \pm SD in μmol cholesterol/g arterial tissue (wet weight). * $P < 0.05$, ** $P < 0.01$. $n = 7$ for the CD and CD1886 groups, and $n = 8$ for the HFSCD and HFSCD1886 groups.

Upregulation of ABCA1 in tissues of NO-1886-treated minipigs

To cast light on the effect of NO-1886 on ABCA1, we investigated expression levels of mRNA and protein for ABCA1 in tissue samples from the liver, retroperitoneal adipose tissue, and aorta of the pigs. ABCA1 mRNA levels were highest in tissues of the HFSCD1886 group compared with pigs in the HFSCD, CD1886, and CD groups. ABCA1 levels in tissues of CD group animals represented the basal expression of ABCA1 in pigs. High-fat/high-sucrose/high-cholesterol feeding increased ABCA1 mRNA levels in tissue samples from the HFSCD group. Moreover, administration of NO-1886 stimulated further higher protein expression of ABCA1 in the HFSCD1886 group; the levels of ABCA1 protein in the liver, retroperitoneal adipose tissue, and aorta of the HFSCD1886 group were 236.9, 18.6, and 108.6% higher, respectively, than in the HFSCD group (Fig. 3). All protein levels were assessed by densitometry with β -actin as a control.

Upregulation of LXR α protein levels in tissues of NO-1886-treated minipigs

ABCA1 expression is dependent on the nuclear receptor LXR α (12), so we next examined whether LXR α was affected by NO-1886. Figure 4 shows that LXR α protein levels were markedly increased in the liver, retroperitoneal adipose tissue, and aorta of pigs from the HFSCD1886 group compared with pigs from the HFSCD, CD1886, and CD groups. High-fat/high-sucrose/high-cholesterol feeding induced increased LXR α protein levels in tissues of HFSCD group animals. Moreover, administration of NO-1886 stimulated more expression of LXR α protein in the HFSCD1886 group than in the HFSCD group. The levels of LXR α protein in the liver of HFSCD1886 group animals were 63.5% higher than in the HFSCD group (Figure 4).

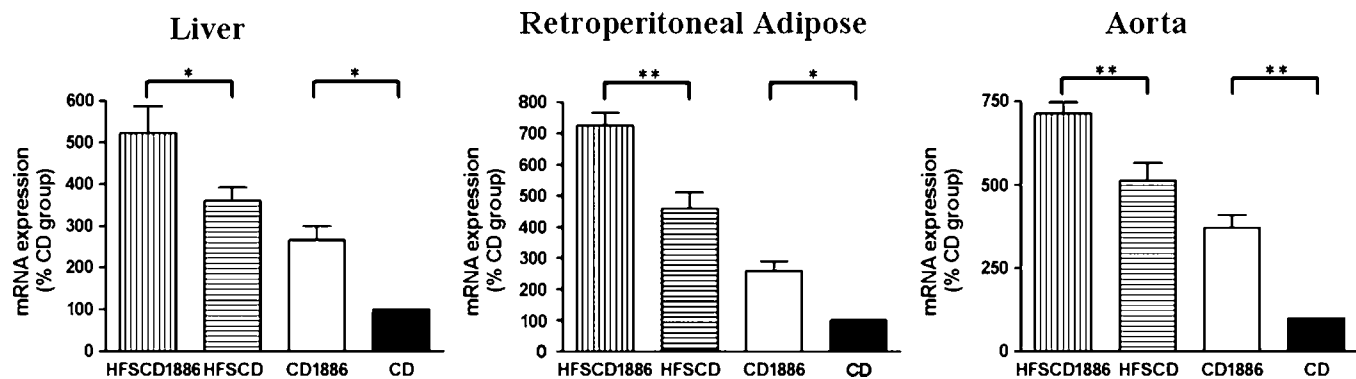


Fig. 3. ABCA1 mRNA levels in liver, retroperitoneal adipose tissue, and aorta as determined by quantitative real-time PCR. Ratios of the ABCA1 to β -actin transcripts are expressed as percentages of the β -actin control. Data are expressed as means \pm SD from three independent experiments, each performed in triplicate. * $P < 0.05$, ** $P < 0.01$.

Moreover, the protein levels of LXR α were highest in the retroperitoneal adipose tissue and aorta of HFSCD1886 group animals compared with pigs from the HFSCD, CD1886, and CD groups. The levels of LXR α protein in

the retroperitoneal adipose tissue of the HFSCD1886 group were 44.9% higher than in the HFSCD group (Fig. 4). Furthermore, in the aorta, LXR α protein was 39.0% higher than in the HFSCD group (Fig. 4). In addition, normal diet

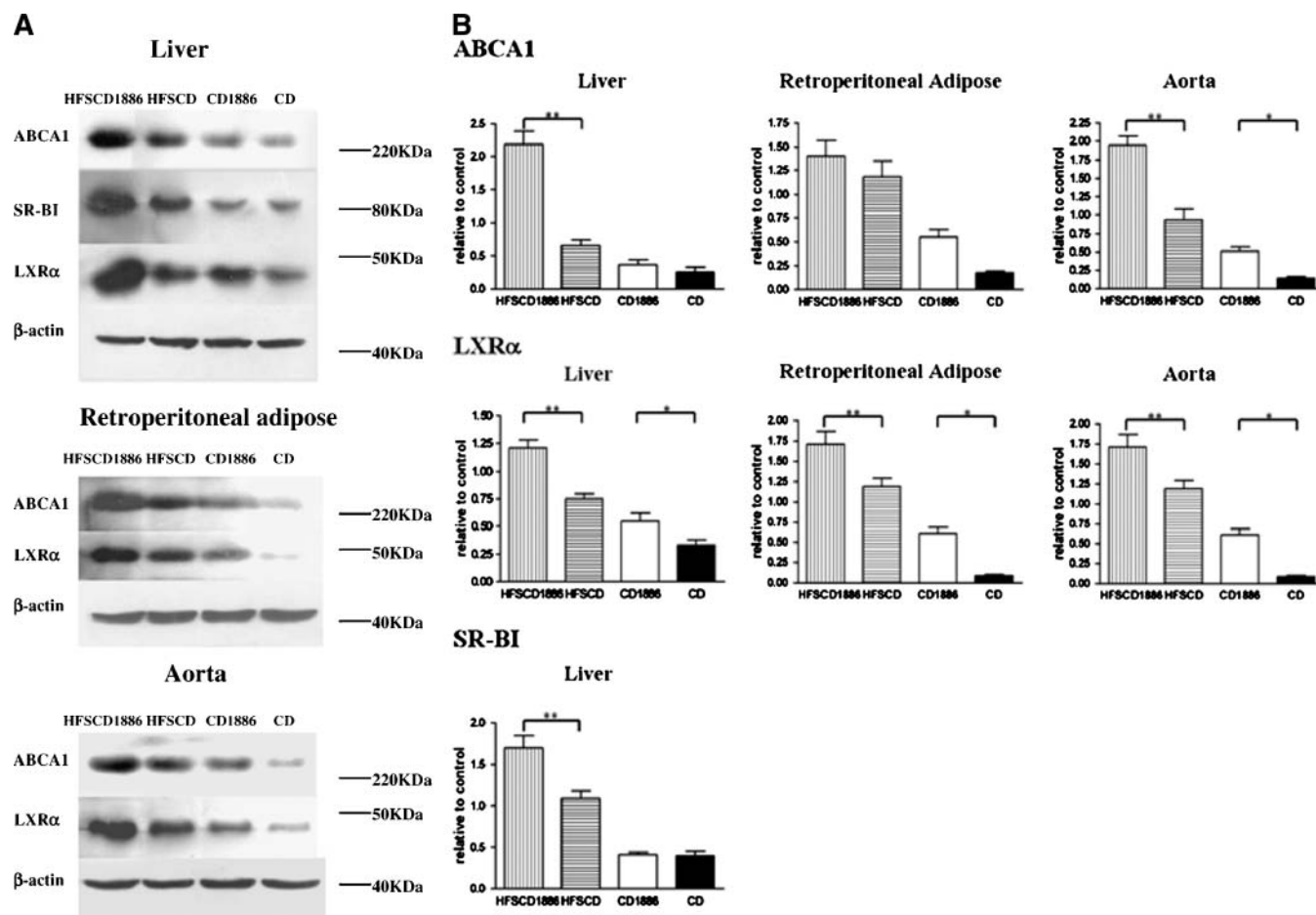


Fig. 4. Western blot analysis of ABCA1, liver X receptor α (LXR α), and scavenger receptor class B type I (SR-BI) protein levels in the liver, retroperitoneal adipose tissue, and aorta. Details of the experiments are described in Materials and Methods. All protein levels were assessed by densitometry with β -actin as a control. A: ABCA1, LXR α , and SR-BI proteins were analyzed from various tissues. B: Statistical graphs of ABCA1, LXR α , and SR-BI protein levels. Data are expressed as means \pm SD from three independent experiments, each performed in triplicate. * $P < 0.05$, ** $P < 0.01$.

plus NO-1886 slightly increased LXR α protein level in the CD1886 group compared with the CD group (Fig. 4). All protein levels were assessed by densitometry with β -actin as a control.

Change of SR-BI protein levels in liver

SR-BI was the first molecularly well-defined cell surface HDL receptor to be described. The liver expresses the highest levels of total tissue SR-BI protein, a finding consistent with the major role of the liver in selective HDL-C uptake. The level of SR-BI protein was increased by NO-1886 in the liver of pigs from the HFSCD1886 group, which was 57.4% higher than in liver of pigs from the HFSCD group. But the levels of SR-BI protein in normal diet groups were lower regardless of supplementation with NO-1886 or not. All protein levels were assessed by densitometry with β -actin as a control.

Plasma LPL and ABCA1 of aorta were independently associated with lesion area

We next performed multivariate linear regression analysis to evaluate the relationship among levels of ABCA1, SR-BI, LPL, and lesion areas of the aorta in HFSCD-fed minipigs (Table 4). The levels of LPL in plasma [standard correlation coefficient (B) = -0.445, P = 0.028] and the levels of ABCA1 in artery (B = -0.390, P = 0.036) were independently associated with lesion area.

DISCUSSION

High cholesterol, high TG, and low HDL-C are important risk factors for coronary artery disease. The TC/HDL ratio can be calculated and used to determine the risk of developing atherosclerosis and consequent coronary artery disease. In this study, we fed minipigs a high-fat/high-sucrose/high-cholesterol diet (HFSCD) to establish dyslipidemia and atherosclerosis and investigated the effects of NO-1886 treatment. Our results showed that feeding HFSCD caused obvious atherosclerotic lesions and increased plasma TC, TG, and FFA levels. Administration of NO-1886 decreased plasma TG, FFA, glucose, and TC/HDL-C ratio and increased plasma HDL-C and apoA-I levels.

HFSCD induced an atherogenic lipoprotein profile, such as hypertriglyceridemia, low HDL, and serious hypercholesterolemia. This characteristic plasma lipid profile

may be attributed to increased production of VLDL-TG and apoB in the liver (15, 16). The availability of substrates, in particular FFA, is thought to be an important factor in increased hepatic VLDL production (17). The complex downregulating the expression of ABCA1 and LXR α would worsen the hypercholesterolemia and serious atherosclerosis observed in the HFSCD group in this study.

It was reported previously that NO-1886 increased LPL mRNA levels, LPL protein mass, and LPL activity in post-heparin plasma and reduced plasma TG levels with concomitant increases of HDL-C levels in animals with lipid disorder. Recently, we found that NO-1886 also had plasma glucose-reducing action in high-fat/high-sucrose diet-induced diabetic rabbits and improved glucose metabolism in high-fat/high-sucrose diet-induced diabetic minipigs by decreasing fat deposits and suppressing plasma tumor necrosis factor- α (1, 18, 19). Here, we found that NO-1886 also increased ABCA1, the gatekeeper for eliminating excess tissue cholesterol (20), in minipigs. Administration of NO-1886 also increased LXR α levels. Multivariate linear regression analysis showed that the level of ABCA1 in artery (B = -0.390, P = 0.036) independently associated with lesion area on the abdominal portion of the aorta. Therefore, we speculate that NO-1886 may play an important role in the "first step" of RCT in vivo and suppress atherosclerosis related to the upregulation of ABCA1.

In this study, we confirmed that hyperlipemia was ameliorated by NO-1886 administration, as found in our previous studies. Furthermore, this time, we observed that NO-1886 increased plasma apoA-I levels. ApoA-I is a prototypical cholesterol acceptor. It is thought that free cholesterol effluxed from macrophage foam cells is transferred to the surface of HDL, where it can be esterified by lecithin:cholesterol acyltransferase and incorporated into the HDL core. Castro et al. (21) suggested that HDL-containing human apoA-I in human apoA-I transgenic mice is an effective participant in the postulated early steps of RCT. Burger and Dayer (22) demonstrated that HDL-associated apoA-I is a specific inhibitor of cytokine production in monocytes-macrophages upon contact with stimulated T-cells. HDL-associated apoA-I might play the role of a constitutive anti-inflammatory factor. The decrease in plasma levels of HDL-associated apoA-I in acute inflammation may be a sign of the possible development of chronic inflammation. Clay et al. (23) suggested that HDL-containing apoA-I mediated the inhibition of vascular cell adhesion molecule-I and E-selectin expression in the development of atherosclerosis. Deckert et al. (24) demonstrated that atherogenic lipoproteins can impair endothelium-dependent arterial relaxation, and circumstantial evidence suggests a beneficial role of plasma HDL and apoA-I in counteracting the endothelium dysfunction. Therefore, the effect of NO-1886 on plasma apoA-I level is considered to be significantly important in protecting against the development of atherosclerosis in the animals studied.

RCT is the process by which peripheral cells release cholesterol to an extracellular acceptor such as HDL, which then mediates cholesterol delivery to the liver for excretion. RCT represents a physiological mechanism by which

TABLE 4. Multivariate linear regression analysis of relationships between the levels of ABCA1, SR-BI, and LPL and the lesion area of the aorta

Independent Variables	Standardized Coefficients	P
Constant	0	<0.001
LPL	-0.445	0.028
ABCA1 (liver)	-0.076	0.572
ABCA1 (adipose)	-0.094	0.425
ABCA1 (artery)	-0.390	0.036
SR-BI (liver)	-0.051	0.725

SR-BI, scavenger receptor class B type I. The dependent variable was lesion area. R^2 = 0.969, F = 61.607, P < 0.001.

peripheral tissues are protected against the excessive accumulation of cholesterol. The first step in RCT is the interaction of the cells with lipoprotein particles, a process that results in both the cellular uptake and release of cholesterol. ABCA1 mediates the cellular efflux of phospholipids and cholesterol to lipid-poor apoA-I and plays a significant role in HDL metabolism and the process of RCT (20). ABCA1's role in the causation of Tangier disease, which is characterized by absent HDL and premature atherosclerosis, has implicated this transporter and its regulators, LXRs, as new candidates potentially influencing the progression of atherosclerosis (12). LXR α and LXR β are members of the nuclear receptor superfamily and intermediates in the cholesterol synthetic pathway. The pivotal role of LXRs in the metabolic conversion of cholesterol to bile acids is well established. It has been confirmed that LXRs regulate a number of target genes involved in both cholesterol and fatty acid metabolism in liver, macrophages, and intestine, such as ABCA1, ABCG5, and ABCG8 (25–27). The observation that LXR α is responsive to fatty acids and is expressed in metabolic tissues suggests that it also plays a general role in lipid metabolism. The results in this study show that long-term feeding of HFSCD increases ABCA1 and LXR α slightly compared with the control diet group. This may be a kind of compensation to resist the toxic effect of excess cholesterol. NO-1886 increased ABCA1 and LXR α markedly in the HFSCD1886 group compared with the HFSCD group. Upregulation of ABCA1 and LXR α by NO-1886 would induce more cholesterol efflux from vessel smooth muscle cells and macrophages, inhibiting the formation of foam cells and reducing aortic fatty streak lesion area. Moreover, adipose cells that specialize in energy storage and contain large intracellular TG-rich lipid droplets are enriched with free cholesterol and express sterol-regulated transcription factors such as LXR. The high cholesterol content in adipose tissue may affect the RCT mediated by HDL. Impairments in this system may be one possible factor favoring the development of atherosclerosis in obesity. The alterations in the first step of RCT are tightly associated with the abdominal distribution of fat mass (28). Upregulation of ABCA1 and LXR α by NO-1886 would induce more cholesterol efflux from retroperitoneal adipose tissue and postpone the development of atherosclerosis.

SR-BI was the first molecularly well-defined cell surface HDL receptor to be described. SR-BI mediates selective HDL-C uptake by the formation of a productive lipoprotein/receptor complex, which requires specific structural domains and conformation states of apoA-I present in HDL particles. The importance of SR-BI in overall HDL-C metabolism and its antiatherogenic activity in vivo has been definitively established by SR-BI gene manipulation in mice (29). Studies of the overexpression of SR-BI clearly demonstrate that hepatic overexpression of SR-BI can be antiatherogenic. This may be attributable to changes in the structures and quantities of circulating lipoproteins or to increases in HDL-C flux to the liver (i.e., increased RCT) (30). In our study, high-fat/high-sucrose/high-cholesterol feeding induced an increase of plasma levels

of HDL and upregulation of hepatic SR-BI expression. SR-BI expression was further enhanced by NO-1886 administration, suggesting that HDL cholesteryl ester clearance, biliary cholesterol content, and transport of cholesterol from the liver into the bile could be increased.

In summary, HFSCD-fed minipigs developed a hyperlipidemic condition with induced distinct fatty streak lesions in the aorta. The administration of the LPL activator NO-1886 significantly increased the levels of plasma HDL-C and apoA-I, and the expression of ABCA1, which contributes to alleviating cholesterol toxicity and ameliorating lipid disorders, results in protection against the development of atherosclerosis. ■■

The authors gratefully acknowledge financial support from Project 973 of China G2000056905 and the National Natural Sciences Foundation of China (Projects 30370675 and 30470720).

REFERENCES

1. Tsutsumi, K., Y. Inoue, A. Shima, K. Iwasaki, M. Kawamura, and T. Murase. 1993. The novel compound NO-1886 increases lipoprotein lipase activity with resulting elevation of high density lipoprotein cholesterol, and long-term administration inhibits atherogenesis in the coronary arteries of rats with experimental atherosclerosis. *J. Clin. Invest.* **92**: 411–417.
2. Tsutsumi, K., Y. Inoue, A. Shima, and T. Murase. 1995. Correction of hypertriglyceridemia with low high-density lipoprotein cholesterol by the novel compound NO-1886, a lipoprotein lipase-promoting agent, in STZ-induced diabetic rats. *Diabetes.* **44**: 414–417.
3. Garfagnini, A., G. Devoto, P. Rosselli, P. Boggiano, and M. Venturini. 1995. Relationship between HDL-cholesterol and apolipoprotein A1 and the severity of coronary artery disease. *Eur. Heart J.* **16**: 465–470.
4. Zampogna, A., M. H. Luria, S. J. Manubens, and M. A. Luria. 1980. Relationship between lipids and occlusive coronary artery disease. *Arch. Intern. Med.* **140**: 1067–1069.
5. Kannel, W. B. 2000. The Framingham Study: its 50-year legacy and future promise. *J. Atheroscler. Thromb.* **6**: 60–66.
6. Fielding, C. J., and P. E. Fielding. 1995. Molecular physiology of reverse cholesterol transport. *J. Lipid Res.* **36**: 211–228.
7. Rothblat, G. H., M. de la Llera-Moya, V. Atger, G. Kellner-Weibel, D. L. Williams, and M. C. Phillips. 1999. Cell cholesterol efflux: integration of old and new observations provides new insights. *J. Lipid Res.* **40**: 781–796.
8. Tall, A. R. 1998. An overview of reverse cholesterol transport. *Eur. Heart J.* **19** (Suppl. A): 31–35.
9. Finking, G., and H. Hanke. 1997. Nikolaj Nikolajewitsch Anitschkow (1885–1964) established the cholesterol-fed rabbit as a model for atherosclerosis research. *Atherosclerosis.* **135**: 1–7.
10. Murase, T., and H. Uchimura. 1980. A selective decline of post-heparin plasma hepatic triglyceride lipase in hypothyroid rats. *Metabolism.* **29**: 797–801.
11. Stappans, I., J. H. Rapp, X. M. Pan, D. A. Hardman, and K. R. Feingold. 1996. Oxidized lipids in the diet accelerate the development of fatty streaks in cholesterol-fed rabbits. *Arterioscler. Thromb. Vasc. Biol.* **16**: 533–538.
12. Folch, J., M. Lees, and G. H. Sloane Stanley. 1957. A simple method for the isolation and purification of total lipids from animal tissues. *J. Biol. Chem.* **226**: 497–509.
13. Rapp, J. H., W. E. Connor, D. S. Lin, T. Inahara, and J. M. Porter. 1983. Lipids in human atherosclerotic plaques and xanthomas: clues to the mechanism of plaque progression. *J. Lipid Res.* **24**: 1329–1335.
14. Singaraja, R. R., V. Bocher, E. R. James, S. M. Clee, L. H. Zhang, B. R. Leavitt, B. Tan, A. Brooks-Wilson, A. Kwok, N. Bissada, et al. 2001. Human ABCA1 BAC transgenic mice show increased high density lipoprotein cholesterol and apoA-I-dependent efflux stim-

- ulated by an internal promoter containing liver X receptor response elements in intron 1. *J. Biol. Chem.* **276**: 33969–33979.
15. Nikkila, E. A., and M. Kekki. 1973. Plasma triglyceride transport kinetics in diabetes mellitus. *Metabolism.* **22**: 1–22.
 16. Cummings, M. H., G. F. Watts, A. M. Umpleby, T. R. Hennessy, R. Naoumova, B. M. Slavin, G. R. Thompson, and P. H. Sonksen. 1995. Increased hepatic secretion of very-low-density lipoprotein apolipoprotein B-100 in NIDDM. *Diabetologia.* **38**: 959–967.
 17. Lewis, G. F. 1997. Fatty acid regulation of very low density lipoprotein production. *Curr. Opin. Lipidol.* **8**: 146–153.
 18. Yin, W., D. Liao, M. Kusunoki, S. Xi, K. Tsutsumi, Z. Wang, X. Lian, T. Koike, J. Fan, Y. Yang, et al. 2004. NO-1886 decreases ectopic lipid deposition and protects pancreatic beta cells in diet-induced diabetic swine. *J. Endocrinol.* **180**: 399–408.
 19. Yin, W., D. Liao, Z. Wang, S. Xi, K. Tsutsumi, T. Koike, J. Fan, G. Yi, Q. Zhang, Z. Yuan, et al. 2004. NO-1886 inhibits size of adipocytes, suppresses plasma levels of tumor necrosis factor-alpha and free fatty acids, improves glucose metabolism in high-fat/high-sucrose-fed miniature pigs. *Pharmacol. Res.* **49**: 199–206.
 20. Oram, J. F., and R. M. Lawn. 2001. ABCA1: the gatekeeper for eliminating excess tissue cholesterol. *J. Lipid Res.* **42**: 1173–1179.
 21. Castro, G., L. P. Nihoul, C. Dengremont, C. de Geitere, B. Delfly, A. Tailleux, C. Fievet, N. Duverger, P. Deneffe, J. C. Fruchart, et al. 1997. Cholesterol efflux, lecithin-cholesterol acyltransferase activity, and pre-beta particle formation by serum from human apolipoprotein A-I and apolipoprotein A-I/apolipoprotein A-II transgenic mice consistent with the latter being less effective for reverse cholesterol transport. *Biochemistry.* **36**: 2243–2249.
 22. Burger, D., and J. M. Dayer. 2002. High-density lipoprotein-associated apolipoprotein A-I: the missing link between infection and chronic inflammation? *Autoimmun. Rev.* **1**: 111–117.
 23. Clay, M. A., D. H. Pyle, K. A. Rye, M. A. Vadas, J. R. Gamble, and P. J. Barter. 2001. Time sequence of the inhibition of endothelial adhesion molecule expression by reconstituted high density lipoproteins. *Atherosclerosis.* **157**: 23–29.
 24. Deckert, V., G. Lizard, N. Duverger, A. Athias, V. Palleau, F. Emmanuel, M. Moisan, P. Gambert, C. Lallemand, and L. Lagrost. 1999. Impairment of endothelium dependent arterial relaxation by high fat feeding in apoE-deficient mice: toward normalization by human apoA-I expression. *Circulation.* **100**: 1230–1235.
 25. Kruit, J. K., T. Plosch, R. Havinga, R. Boverhof, P. H. Groot, A. K. Groen, and F. Kuipers. 2005. Increased fecal neutral sterol loss upon liver X receptor activation is independent of biliary sterol secretion in mice. *Gastroenterology.* **128**: 147–156.
 26. Hoekstra, M., J. K. Kruijt, M. Van Eck, and T. J. Van Berkel. 2003. Specific gene expression of ATP-binding cassette transporters and nuclear hormone receptors in rat liver parenchymal, endothelial, and Kupffer cells. *J. Biol. Chem.* **278**: 25448–25453.
 27. Repa, J. J., K. E. Berge, C. Pomajzl, J. A. Richardson, H. Hobbs, and D. J. Mangelsdorf. 2002. Regulation of ATP-binding cassette sterol transporters ABCG5 and ABCG8 by the liver X receptors alpha and beta. *J. Biol. Chem.* **277**: 18793–18800.
 28. Autran, D., B. Guerci, J. L. Paul, P. Moulin, B. Verges, V. Durlach, and A. Girard-Globa. 2001. Basal and postprandial serum-promoted cholesterol efflux in normolipidemic subjects: importance of fat mass distribution. *Metabolism.* **50**: 1330–1335.
 29. Trigatti, B. L., M. Krieger, and A. Rigotti. 2003. Influence of the HDL receptor SR-BI on lipoprotein metabolism and atherosclerosis. *Arterioscler. Thromb. Vasc. Biol.* **23**: 1732–1738.
 30. Rigotti, A., H. E. Miettinen, and M. Krieger. 2003. The role of the high-density lipoprotein receptor SR-BI in the lipid metabolism of endocrine and other tissues. *Endocr. Rev.* **24**: 357–387.